Acta Chemica Scandinavica, 1996: 50: 862–870
Printed in UK – all rights reserved

ACTA
CHEMICA SCANDINAVICA
ISSN 0904–213X

Surface Models for the Adsorption of a Calcium β-Diketonate Complex on Calcium Sulfide

Maria José Calhorda,[a,b,*] Luís F. Veiros[b,c] and Lauri Niinistö[d]

[a]ITQB, R. da Quinta Grande, 6, Apart. 127, P-2780 Oeiras, Portugal, [b]IST, Av. Rovisco Pais, P-1096 Lisboa Codex, Portugal, [c]CQE, P-1096 Lisboa Codex, Portugal and [d]Laboratory of Inorganic and Analytical Chemistry, Helsinki University of Technology, FIN-02150 Espoo, Finland

Calhorda, M. J., Veiros, L. F. and Niinistö, L., 1996. Surface Models for the Adsorption of a Calcium β-Diketonate Complex on Calcium Sulfide. – Acta Chem. Scand. 50: 862–870. © Acta Chemica Scandinavica 1996.

Extended Hückel tight-binding calculations were used to study the bonding modes of β-diketonate precursor complexes to three possible adsorption sites of the S(111) surface of calcium sulfide, in order to study gas phase deposition of thin layered calcium sulfide. Molecular models were also used for comparison. The three-fold site seems to be favored for adsorption, as stronger calcium–surface bonds are formed. The bonding occurs through donation from surface sulfur lone pairs into empty orbitals of the calcium complex. These acceptor orbitals are mainly located on the calcium atoms and have a strong calcium–oxygen antibonding character. Though the large energy difference between calcium and sulfur orbitals is responsible for weak interactions, many calcium–oxygen antibonding levels become also calcium–sulfur bonding, and their energy falls below the Fermi level. The Ca–O bonds weaken, thus activating the adsorbed β-diketonate complex toward loss of the ligand.

Gas-phase deposition of alkaline-earth-containing thin films to be used, for example, in electroluminescent displays and superconductors,[1,2] is a rapidly growing area of research and technology. In addition to chemical vapor deposition (CVD), a more sophisticated deposition process, namely atomic layer epitaxy (ALE), can be used.[3] The choice of precursors is, however, in both cases limited, and only the β-diketonate-type complexes of the alkaline earth metals have a sufficient volatility for practical purposes. The most commonly used complexes are those formed by the thd ligand (thd= 2,2,6,6-tetramethyl-3,5-heptadione), also abbreviated as dpm (dipivaloylmethanate). Unfortunately, the stability of the complexes is low both in the solid state under storage and in the gas phase, and therefore various ways have been devised to overcome this stability problem including an *in situ* synthesis.[4] Nevertheless, the ALE process produces good quality thin films[5] also with alkaline earths, especially when the experimental conditions are carefully optimized.[6]

The formation of sulfide thin films from the β-diketonate precursors and hydrogen sulfide involves alternate pulsing of the reactants into the reactor, the pulses being separated by an inert gas purge. The chemisorbed β-diketonate precursor reacts on the surface with H_2S, whereupon the metal–oxygen bond is broken and replaced by the metal–sulfur bond. If the reaction is complete, no carbon or oxygen residues are left in the film. While the formation of ZnS thin films by ALE from $ZnCl_2$ and H_2S has been modeled,[7] so far no attempts have been made to describe theoretically the more complex ALE processes involving the bulky β-diketonate ligands. There are, however, experimental IR and EXAFS data on the adsorbed Ca(thd) and Cu(thd) precursors on hydroxylated silicon dioxide surfaces which indicate that the surface complexes are stabilized by the ligand–surface interaction, and the mechanism appears thus to be independent of the metal ion.[8]

The adsorption of β-diketonate calcium complexes, modeled after [Ca(thd)$_2$], on the sulfur (111) surface of calcium sulfide, will be studied in this work, using the extended Hückel method[9] with the tight-binding approach,[10] in order to gain more knowledge on the preferred adsorption sites, the complex–surface bonding mode and the surface activation process. This should help us to understand the ALE film growth mechanism involving β-diketonate complexes.

Results and discussion

The surface. CaS has the rock-salt structure, with two face-centered cubic interwoven nets, and a lattice para-

* To whom correspondence should be addressed.

meter $a = 5.702$ Å. One net is occupied by the Ca^{2+} cations and the other by the S^{2-} anions.[11]

The (111) surface is formed by a triangular net of sulfur atoms, the S–S distance being 4.03 Å, and is depicted in Fig. 1, showing only the surface atoms in a top view, and the four layers used in the model surface in a side view.

Two layers of sulfur and two of calcium, alternately disposed, were chosen in order to model the growth of a film. Though three layers have often been used in surface calculations of this type,[12] so as to have a good balance between a reliable description of the surface and an acceptable size for the calculation, a different number was thought more appropriate in this case, to keep the surface neutral. Another factor to take into account, concerning the size of the calculations, is the choice of the unit cell, which should be as small as possible.[13] The limitation, however, arises from the need to avoid strong repulsive interactions between the adsorbed molecules. A relatively big unit cell may be used in order to keep adjacent molecules at suitable distances, as in the present study. Only one unit cell is shown in Fig. 1.

Three different adsorption modes were studied for a model β-diketonate complex of calcium over the S(111) surface of CaS. The calcium atom was either on top of a sulfur atom, bridging two sulfurs, or on a three-fold site bridging three sulfurs. The Ca–S distance was always kept constant at 2.85 Å, the experimental distance in CaS. Our analysis will begin with the isolated adsorbate molecule, the β-diketonate complex, and its bonding mode to some simple molecular models. The results will be used in interpreting the binding mode between the adsorbate and the surface.

The calcium complex and its electronic structure. The most commonly used precursor for ALE of CaS is $[Ca(thd)_2]$, where thd is shown in **a**.[4] The bulky ^{t}Bu groups were replaced by H in the model, and the resulting ligand denoted as thd', **b**. The use of such a model reduces the size of the calculation, without significantly affecting the bonding capabilities of the ligand and of the complex.

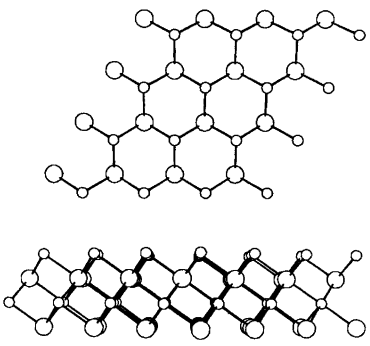

Fig. 1. The S(111) surface of CaS: top view (above) and side view (below). Only the sulfur top layer (small circles) and the adjacent Ca layer are shown, for clarity, on the top view.

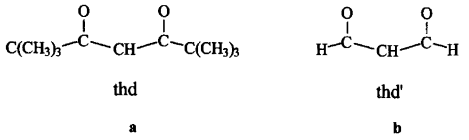

The $[Ca(thd')_2]$ complex is given in **c**. The two limiting geometries are square planar and tetrahedral, the last one being the more stable, according to our calculations, by only 0.04 eV.

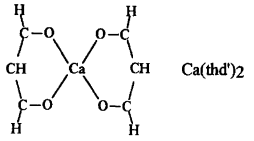

The lack of preference for a square planar environment is normal for a d^0 species,[14] but as the complex should more easily approach the surface as a planar molecule liable to distortion rather than a tetrahedral species, we started by studying the electronic structure of that slightly less stable form. The interaction diagram between the two ligands and the calcium atom is shown, in a very simplified form, in Fig. 2.

Three of the Ca–O bonds are of σ type and electrons from the combinations of oxygen orbitals, a_g, b_{3u}, b_{2u},

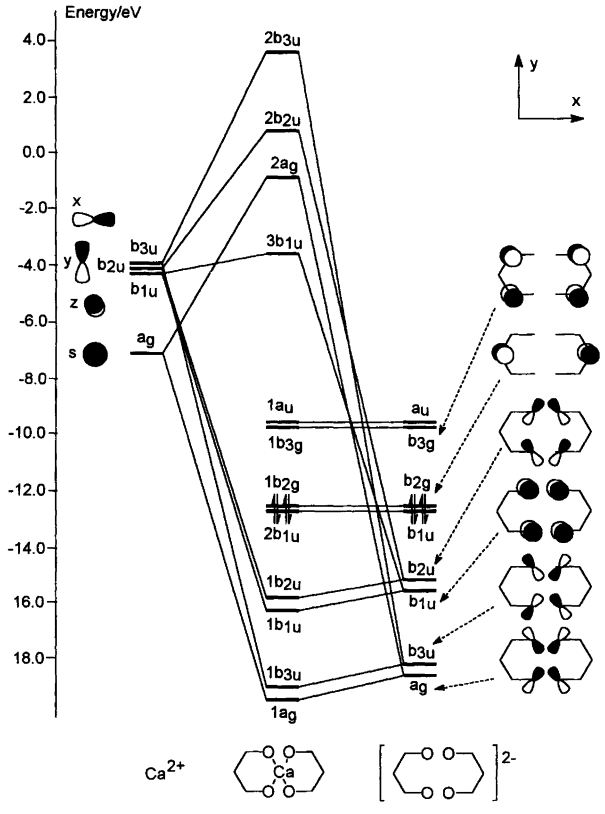

Fig. 2. Interaction diagram between two thd' ligands and one calcium atom in a square planar arrangement (only the most relevant contributions to the thd' fragment orbitals are shown on the right side).

are donated into empty s, x and y of Ca. The last is a π type Ca–O bond: the Ca z orbital receives electrons from a π orbital of the ligand (b_{1u}). These interactions are shown in the diagram of Fig. 2, as well as the frontier orbitals of the complex. Both the HOMO and LUMO are formed by one pair of orbitals each, at very similar energies, and are separated by 2.5 eV.

Each of these pairs is composed by the symmetrical and antisymmetrical combinations of π orbitals of the thd′ ligand. The HOMO ($1b_{2g}$, $2b_{1u}$) has as main contributors z orbitals of the central carbons, while the LUMO ($1a_u$, $1b_{3g}$) is essentially localized in the z orbitals of the carbonyl carbons. These are all non bonding orbitals, which play no role in bonding either to thd′ or to sulfur. One member of each pair (HOMO, $2b_{1u}$, and LUMO, $1b_{3g}$) is depicted in Fig. 3 in a three-dimensional representation.[15]

The calcium and thd′ fragment orbitals have very distant energies, and the contribution of calcium orbitals to the bonding molecular orbitals is quite small, while the antibonding mo's are mostly calcium in character. This is also reflected by a relatively small overlap population between fragments (0.33) and a high positive charge in the metal (1.66).

Molecular models for the surface. The possible coordination modes of [Ca(thd′)$_2$] to one, two or three sulfur atoms in H_2S are now addressed. As the CaS surface is neutral, a H_2S group was used for each coordinating sulfur atom, so that the model for the top adsorption will be the complex [Ca(thd′)$_2$(SH_2)], where calcium has coordination number 5.

Both square pyramidal and trigonal bipyramidal structures were studied, and the more important parameters optimized. As the energies are similar, the square pyramidal form, more appropriate for an adsorption geometry on the surface, was analysed in more detail. In its optimized structure (**d**), the angle between the two planes containing the thd′ ligand goes from 180° in the initial square planar compound to 117°, the ligands staying planar. No bond lengths were allowed to change. The H_2S group stays on the plane bisecting the other two.

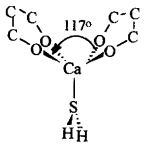

d

The calcium atom is now out of the plane defined by the four oxygen atoms. The new Ca–S bond forms through donation of electrons from the sp sulfur lone pair into what is mainly the z orbital of calcium, with some s mixed in and deriving from $3b_{1u}$ in Fig. 2, still empty after the distortion away from square planar (Fig. 4). Notice that the levels of [Ca(thd′)$_2$] sketched on the right side of Fig. 4 differ from those of the square planar complex essentially in the mixing between the s-based and the z-based molecular orbitals of the complex, as a result of the loss of the horizontal symmetry plane. The same labels will, however, be kept, to make easier the identification of the relevant levels. The frontier orbitals are not affected by the distortion.

The bonding molecular orbital has a greater contribution of sulfur, while the antibonding one is mainly located on the calcium atom (note the mixing of s in the pure z orbital of the square planar geometry, $3b_{1u}$). There is only a small electronic transfer from sulfur to calcium (0.25 electrons). The interaction between one sulfur lone

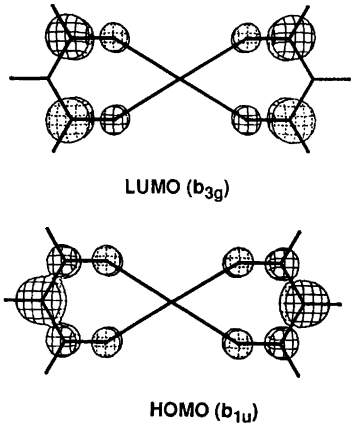

Fig. 3. The HOMO ($2b_{1u}$, below) and the LUMO ($1b_{3g}$, above) of a square planar [Ca(thd′)$_2$] complex.

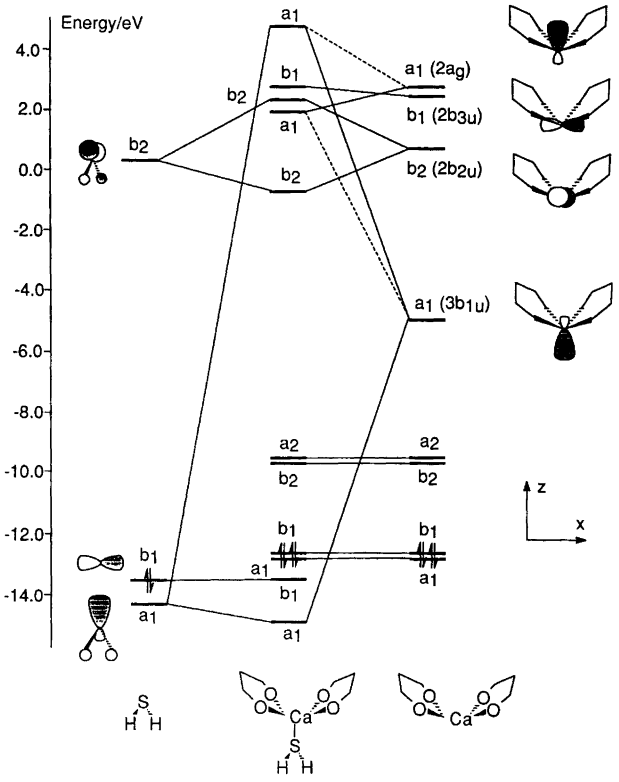

Fig. 4. Interaction diagram between [Ca(thd′)$_2$] and one H_2S group.

pair, perpendicular to the H–S–H plane, and the x orbital of calcium is negligible. The energies of the levels stay unchanged and the overlap population between fragment orbitals is only 0.001. The frontier orbitals of this pentacoordinate complex are still the same as in the parent square planar complex with a similar HOMO–LUMO gap.

The Ca–S overlap population is 0.354, while the Ca–O overlap population dropped to 0.123, from 0.135 in the square planar complex, owing to the population of the new Ca–S bonding orbital which is simultaneously Ca–O antibonding. The charge on the calcium atom becomes lower (1.43) following electron donation from the sulfur atom.

In the second model, two H_2S groups mimic a two-fold bridging environment of the surface and Ca increases its coordination number to 6. Some angles were optimized for the two current geometries, trigonal prismatic and octahedral, the octahedron being more stable by 0.05 eV. A distorted octahedral structure was observed for $[Ca(acac)_2(H_2O)_2]$.[16] The trigonal prismatic structure is, however, more suitable for modeling the adsorption on the surface, and its low energy indicates that its existence is likely.

In the optimized structure, the two thd′ ligands remain planar, but the angle between them narrows to 100°. The S–Ca–S plane bisects their planes and the S–Ca–S angle is 95°. The H–S–H planes are perpendicular to the S–Ca–S plane, as represented in **e**.

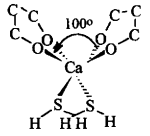

e

The interaction diagram (not shown) is very similar to that represented in Fig. 4. As two H_2S ligands coordinated to calcium, two new bonds are formed and two empty orbitals of the $[Ca(thd')_2]$ fragment, $3b_{1u}$ and $2b_{2u}$, receive electrons coming from the symmetric and antisymmetric combinations of sulfur lone pairs. The geometry of $[Ca(thd'_2]$ is again slightly different, but the energy and nature of their frontier orbitals do not change significantly.

The Ca–S overlap population (0.307) is slightly smaller than for the previous model, but now two bonds are formed. The occupation of two Ca–O antibonding levels ($3b_{1u}$ and $2b_{2u}$) results in even weaker Ca–O bonds (overlap population 0.119).

In the last model the calcium complex interacts with three sulfur atoms in order to mimic a three-fold adsorption site. Some geometry optimization had to be made on a basic structure which may be called a 'bent piano stool', shown in **f** in two views. The two thd′ ligands point upwards, as before, but the angle between their planes is now only 90°. The Ca and the three sulfur atoms define a triangular pyramid pointing in the opposite direction. The S–Ca–S angle was optimized at 89°, and the best relative orientation of the two parts of the molecule was found to be as in **f**.

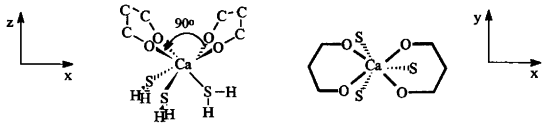

f

In this new heptacoordinated calcium complex, three empty, mainly p, calcium orbitals, $3b_{1u}$, $2b_{2u}$ and $2b_{3u}$, are used to receive electrons from the combinations of the three sulfur lone pairs. Only 0.51 electrons are transferred to the metal atom. The three new Ca–S overlap populations are again slightly smaller (0.273, 0.276), and the Ca–O bonds weaken more significantly (OP 0.105, 0.110).

In conclusion, the two thd′ ligands can reorient relative to each other with small influence on the energy and composition of the orbitals of the resulting $Ca(thd')_2$ fragment. Both the HOMO and LUMO are always π orbitals localized on the thd′ ligand. The optimized geometries are essentially determined by the steric requirements existing in each geometry, and the energy differences between different structures are within 0.15 eV. A small amount of sulfur to calcium electron transfer takes always place, increasing with the number of coordinated sulfur atoms. The Ca–O bonds are simultaneously weakened.

The complex adsorbed on the CaS surface. Three adsorption sites, S1, S2 and S3, simulate the top adsorption of $[Ca(thd')_2]$ on one sulfur, on a bridging site, and on a three-fold site of the S(111) surface of CaS. Two different limiting orientations were probed for both S1 and S2, but as the results were essentially the same, only one of them will be discussed. Top views from the unit cells[13] describing the three structures are given in Fig. 5 (only the surface S layer and the complex are shown for the top view). The local geometries are the same as in the corresponding molecular model.

In order to study the bonding between the calcium complex and the sulfur surface in each site, several indicators can be used.[13] Among the most important ones are the crystal orbital overlap populations, which give an indication about the strength of the new bonds formed and how the old bonds, inside both the surface and the adsorbate, are changed. The binding energy, BE, defined as the difference between the energy of the composite system (surface plus adsorbate) and the sum of the energies of the isolated CaS slab and the square planar $[Ca(thd')_2]$, is useful as an indicator, but is not very reliable for the type of calculations employed. A positive binding energy means an attractive interaction between the two layers. The energy of an isolated molecule of the complex was taken as reference, though the energy calculated for each adsorbate slab was higher

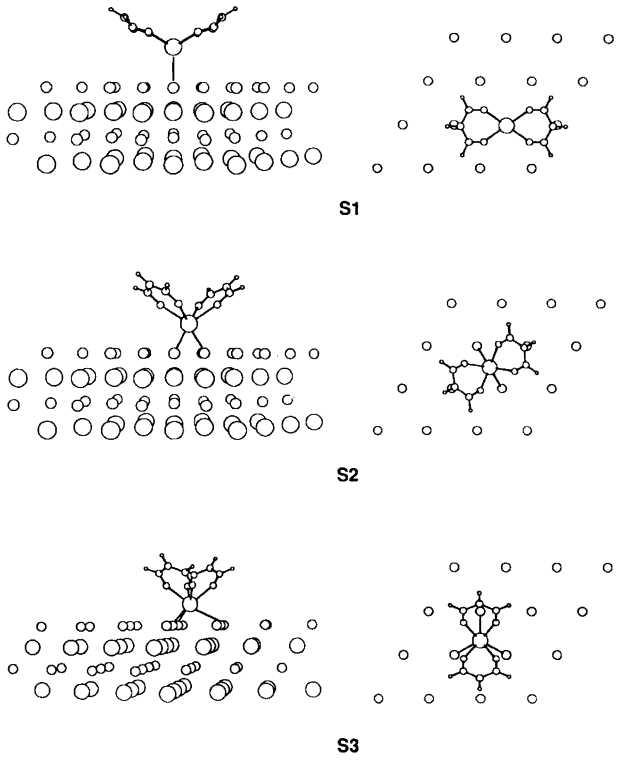

Fig. 5. Unit cells describing the adsorption geometries of [Ca(thd')$_2$] over CaS for the three sites S1, S2 and S3 (side and top view). Only the surface sulfur layer of CaS and the adsorbate are shown for the top view.

(0.05, 0.12 and 0.20 eV for S1, S2 and S3, respectively) as a result of the distortion away from square planar. On the other hand, owing to the low coverage, the molecules are relatively far apart, avoiding repulsive interactions. Charges in some atoms, overlap populations, and binding energies are collected in Table 1.

The three-fold adsorption site appears as the most favorable, as three strong sulfur–calcium bonds are formed, although the binding energy is higher for the bridging site. Although each of them is weaker than those formed on the lower multiplicity sites, the set of three gives rise to a global stronger bonding mode. The fact that three surface sulfur atoms are involved in bonding in S3 leads to more disruption of bonds inside the CaS surface than for both S2 and S1. This is reflected in the weakened Ca_{surf}–S_{surf} bonds calculated, 0.222, compared to 0.237 in the clean surface.

More interesting is certainly what happens to the bonds inside the adsorbed [Ca(thd')$_2$], as this determines the activation of this molecule. As can be seen from Table 1, the Ca–O bonds become weaker upon adsorption and while going from S1 to S2 and S3, suggesting that they should be broken more easily once the complex is adsorbed in the surface than on the gaseous phase prior to adsorption.

This behavior parallels what was found in the molecular models and its causes can be traced to the nature of the adsorbate/surface interaction. Total densities of states[13] are shown in Fig. 6 for the clean CaS surface (left) and the three different composite structures S1, S2 and S3. Projections of all the states belonging to [Ca(thd')$_2$], when the molecule is adsorbed in each of the three sites, are included in the other three panels (dark shadowed area).

The total density of states for the CaS surface, on the top left, shows a concentration of levels below the Fermi level, between −12.5 and −14.5 eV, which are the Ca–S bonding levels, similar to the Ca–S bonding molecular orbitals described in Fig. 4. The antibonding levels start to be seen above −8 eV.

The peaks of the adsorbate are shifted relative to their energies in the isolated species for any of the three sites. This indicates an interaction with the surface, pushing some levels up, some levels down. As the complex on the surface is slightly distorted relative to the initial square-planar geometry, we compare the projections with the total density of states of one layer of adsorbates having the same geometry as in each of the three sites. Only the coordination effect is thus analysed, while that of the distortion is eliminated. The results are depicted in Fig. 7. The upper view shows the total density of states for isolated layers of the adsorbate having the same geometries as in S1, S2 or S3. The more important peaks are assigned. The fact that they are thin peaks indicates no interaction between adjacent molecules. For instance, the peaks for S1 are observed at the same energies as the thd' fragment orbitals on the right side of Fig. 4. The lower view of Fig. 7 shows the projection of all the states of the same adsorbate layers after they

Table 1. Binding energies, overlap populations and charges for [Ca(thd')$_2$] adsorbed on the S(111) surface of CaS in three different sites, S1, S2 and S3, and for the respective molecular models (values in parenthesis).

Geometry	S1	S2	S3	Clean CaS or [Ca(thd')$_2$]
BE eV	0.72 (1.05)	0.95 (1.62)	0.86 (1.87)	—
OP Ca–S_{surf}	0.297 (0.354)	0.237 (0.307)	0.207 (0.275)	—
OP Ca_{surf}–S_{surf}	0.231	0.224	0.222	0.237
OP Ca–O	0.131 (0.133)	0.124 (0.130)	0.118 (0.126)	0.135
OP C–O	0.815 (0.820)	0.814 (0.815)	0.814 (0.814)	0.815
OP C–C	1.080 (1.080)	1.080 (1.080)	1.080 (1.080)	1.080
Charge Ca	1.47 (1.43)	1.38 (1.30)	1.34 (1.21)	1.66
Charge S_{surf}	−1.36 (0.02)	−1.42 (-0.02)	−1.45 (−0.04)	−1.56

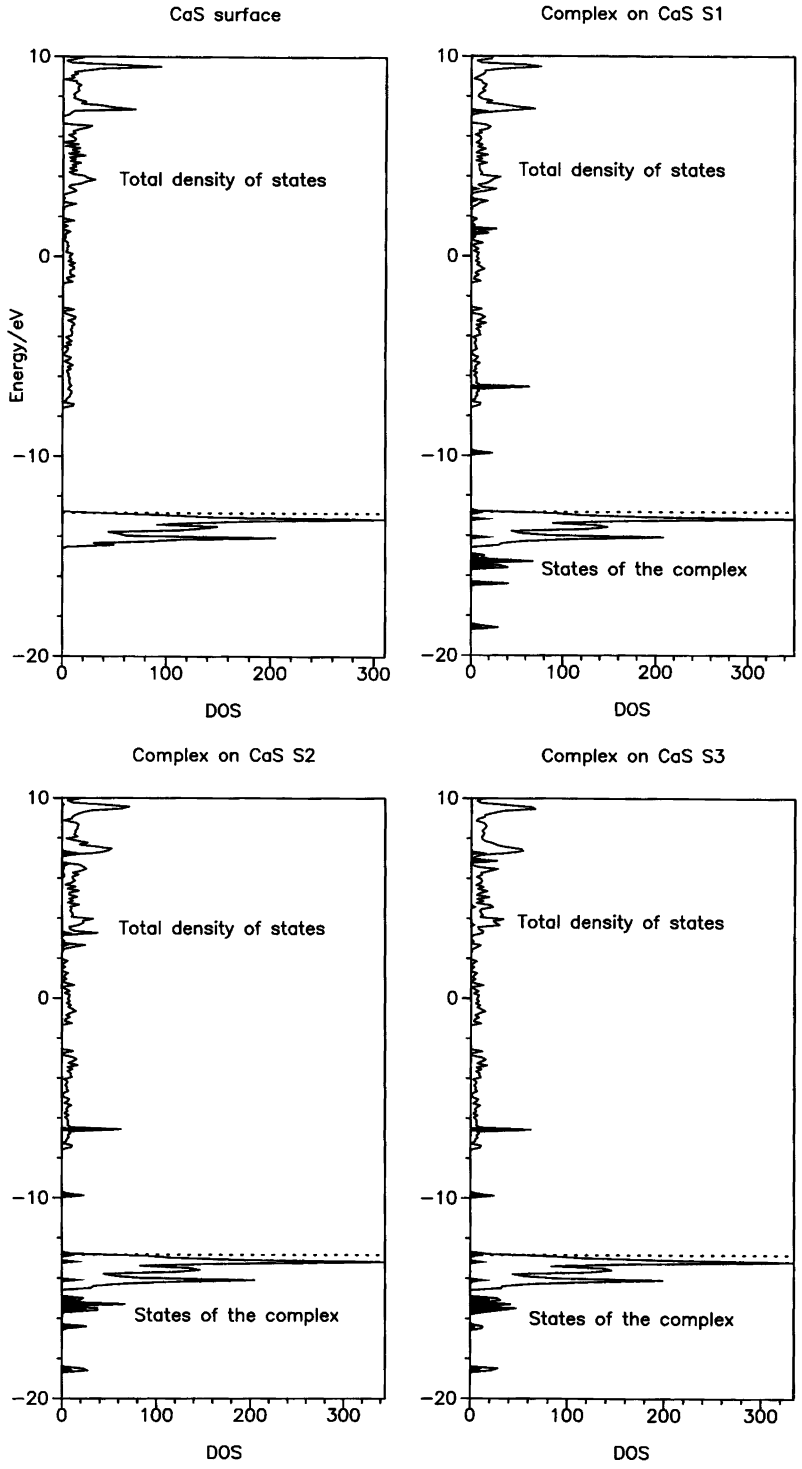

Fig. 6. Total densities of states for the clean CaS surface (upper left) and the same surface covered with $[Ca(thd')_2]$ in three different adsorption sites, S1, S2 and S3. The states of the adsorbate correspond to the shadowed curves. The Fermi level is represented by the dotted horizontal line.

have interacted with the sulfur atoms of the surface. The $3b_{1u}$ peak, for instance, disappears completely from its initial position for all sites. Other peaks, such as the HOMO and the LUMO, remain as sharp peaks with the same energy they had before adsorption.

Up to three levels of the complex are significantly altered upon adsorption, depending on the site. They are the Ca–O antibonding levels already shown to play the major role in bonding to H_2S units in the molecular models and labeled as $3b_{1u}$, $2b_{2u}$ and $2b_{3u}$, which are projected in Fig. 8. For the S1 site, only one Ca–S bond is formed and only $3b_{1u}$ (solid line) is shifted. The other

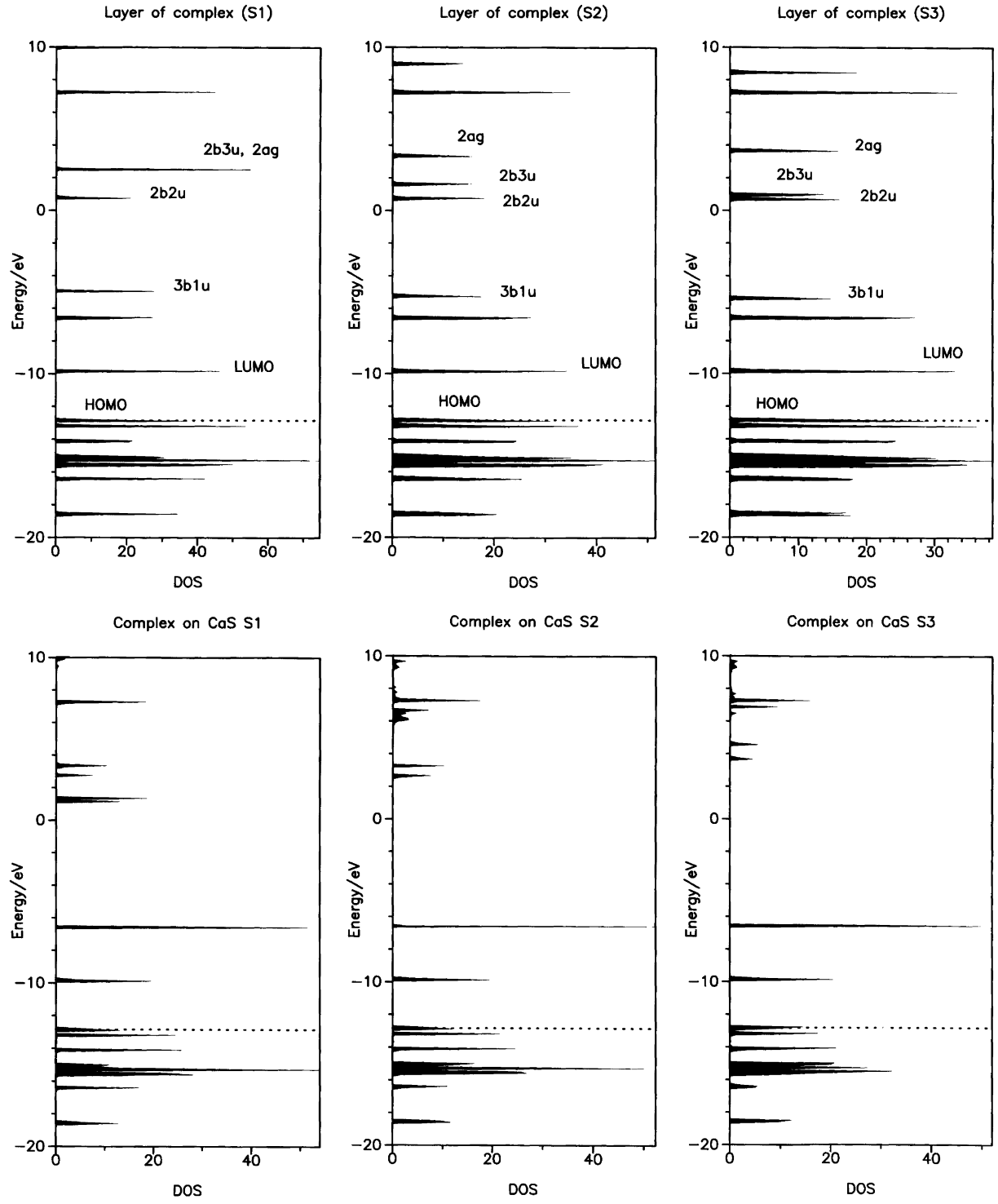

Fig. 7. Total density of states of layers of [Ca(thd')$_2$] with the same geometries as in S1, S2 and S3 (above) and projections of the states of the complex adsorbed in S1, S2 or S3 sites of CaS (below). The Fermi level is represented by the dotted horizontal line.

two peaks (under the black areas) remain sharp and their energy does not change. The formation of two Ca–S bonds in S2 requires the involvement of two acceptor orbitals of the complex, $3b_{1u}$ (solid line) and $2b_{2u}$ (dotted line). The $2b_{2u}$ level has, before adsorption, essentially the same energy for the three layers. After the complex adsorbs on the S2 site, its center of gravity is pushed up ca. 7 eV. Finally, for S3, the three levels must be used in order to form the three Ca–S bonds. $3b_{3u}$ is also seen to shift to higher energies.

The initial single peak originates two main groups of peaks. One at low energy -12.5 to -14.5 eV) includes

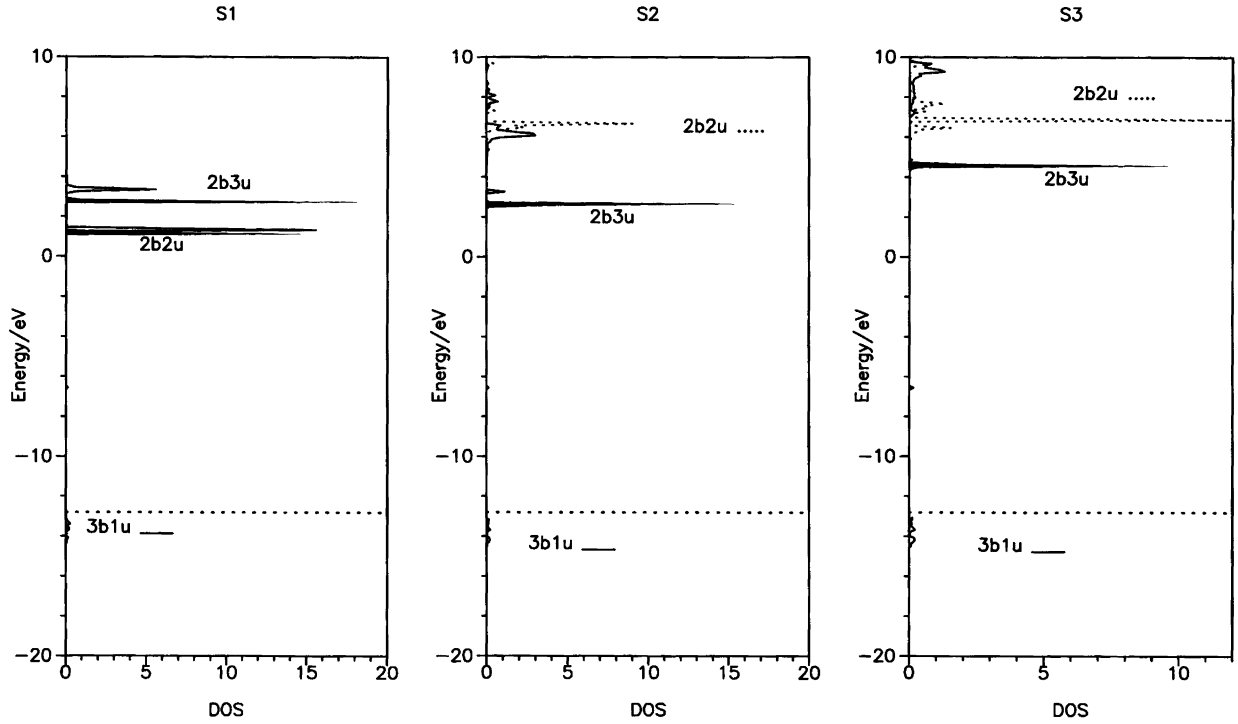

Fig. 8. Projections of the three levels, $3b_{1u}$, $2b_{2u}$ and $2b_{3u}$, of the [Ca(thd')$_2$] complex adsorbed on each of the three sites. The $3b_{1u}$ level is always represented by the solid line. The Fermi level is represented by the dotted horizontal line.

bonding Ca–S_{surf} levels, and shows the effective participation of calcium in these bonds. The high-energy region, where Ca–S antibonding levels are located, has an increasing number of peaks as the multiplicity of the site increases and a larger number of Ca–S_{surf} bonds forms. This is best seen for the $3b_{1u}$ level, which interacts more strongly with the sulfur orbitals, owing to a better overlap.

The calcium atom makes adsorbate–surface bonds using Ca–O antibonding orbitals of the complex fragment. Many of them are pushed down by the interaction, falling below the Fermi level, and being thus filled. The Ca–O bonds become weaker, only slightly for S1, more and more for S2 and S3. This should enable the bond to break more easily after adsorption, as is required for the thin film to grow.

It is interesting that the complex prefers to adsorb at the three-fold site. This leaves the calcium atom in exactly the position it would occupy if it were part of CaS slab from the beginning. A structurally perfect film can therefore grow.

Conclusions

The calcium atom makes adsorbate–surface bonds using orbitals of the complex fragment which are Ca–O antibonding, both for the molecular model complexes and for the S(111) surface of calcium sulfide. The Ca–O bonds become weaker upon adsorption, in spite of the relatively weak interactions and small populations of the Ca–O σ* levels. The Ca–O bonds should, however, break more easily after activation by the surface. The three-fold site, besides being preferred for adsorption, is the one leading to the formation of a perfect overlayer of Ca atoms.

A further observation can be made concerning the removal of the thd' ligands from the complex, which is a necessary step for thin film growth. The breaking of the calcium–oxygen bonds is further induced by electrophilic attack of H_2S, transferring one proton to the central atom of the ligand. This is indeed a favored position of attack, as seen in the HOMO of the calcium complexes. The central carbom atom always possesses a negative charge (ca. −0.21) for all the models studied.

Appendix

All the calculations were done using the extended Hückel method[9] with the tight-binding approach[10] and modified H_{ij} values.[17] The basis set for the calcium and sulfur atoms consisted of *n*s and *n*p orbitals, which were described by single Slater-type wavefunctions. The parameters used for Ca were (H_{ii}/eV, ζ): 4s −7.00, 1.200; 4p −4.00, 1.200. Standard parameters were used for the other atoms.

Idealized models were used in all calculations. They were based on the experimentally observed structure of β-diketonate complexes of calcium and calcium sulfide. The following distances (in Å) were used for the [Ca(thd')$_2$] complex: Ca–S 2.85, Ca–O 2.33, C–O 1.28, C–C 1.41, C–H 1.09, S–H 1.30. The unit cell taken to model the CaS surface consisted of four layers,

S–Ca–S–Ca, the top layer being the S(111) surface and containing 16 atoms (4×4). The coverage was always 1/16. A set of 16 *k*-points in the irreducible wedge of the Brillouin zone was used.[18]

References

1. Niinistö, L. and Leskelä, M. *Appl. Surf. Sci. 82/83* (1994) 454.
2. Leskelä, M., Mölsä, H. and Niinistö, L. *Supercond. Sci. Technol. 6* (1993) 627.
3. Suntola, T. *Mater. Sci. Rep. 4* (1989) 261.
4. Soininen, P., Leskelä, M., Nykänen, E. and Niinistö, L. *Chem. Vapor Deposition. 2* (1996) 69.
5. Tammenmaa, M., Antson, H., Asplund, M., Hiltunen, L., Leskelä, M., Niinistö, L. and Ristolainen, E. *J. Cryst. Growth 84* (1987) 151.
6. Rautanen, J., Leskelä, M., Niinistö, L., Nykänen, E., Soininen, P. and Utriainen, M. *Appl. Surf. Sci. 82/83* (1994) 553.
7. Pakkanen, T., Nevalainen, V., Lindblad, M. and Makkonen, P. *Surf. Sci. 188* (1987) 456.
8. Sekine, R., Kawai, M., Asakura, K., Hikita, T. and Kudo, M. *Surf. Sci. 278* (1992) 175.
9. (a) Hoffmann, R. *J. Chem. Phys. 39* (1963) 1397; (b) Hoffmann, R., Lipscomb, W. N. *J. Chem. Phys. 36* (1962) 2179; *36* (1962) 2872.
10. (a) Whangbo, M.-H. and Hoffmann, R. *J. Am. Chem. Soc. 100* (1978) 6093; (b) Whangbo, M.-H., Hoffmann, R. and Woodward, R. B. *Proc. R. Soc. Chem., Ser. A 23* (1979) 366.
11. Flahaut, J., Domange, L. and Patrie, M. *Bull. Chem. Soc. Fr.* (1962) 2048.
12. (a) Zheng, C., Apeloig, Y. and Hoffmann, R. *J. Am. Chem. Soc. 110* (1988) 749; (b) Saillard, J.-Y. and Hoffmann, R. *J. Am. Chem. Soc. 106* (1984) 2006.
13. (a) Hoffmann, R. *Rev. Mod. Phys. 60* (1988); (b) Hoffmann, R. *Solids and Surfaces: A Chemist's View of Bonding in Extended Structures*, VCH, Weinheim 1988.
14. Albright, T. A., Burdett, J. K. and Whangbo, M.-H. *Orbital Interactions in Chemistry*, Wiley, New York 1985.
15. Mealli, C. and Proserpio, D. M. *J. Chem. Ed. 67* (1990) 39.
16. Sahbari, J. J. and Olmstead, M. M. *Acta Crystallogr., Sect. C39* (1983) 208.
17. Ammeter, J. H., Bürgi, H.-B., Thibeault, J. C. and Hoffmann, R. *J. Am. Chem. Soc. 100* (1978) 3686.
18. Ramirez, R. and Böhm, M. C. *J. Quantum Chem., 30* (1986) 391.

Received 3 November, 1995.